Dalton Transactions

Accepted Manuscript

ROYAL SOCIETY OF CHEMISTRY

www.rsc.org/dalton

Journal Name

COMMUNICATION

Mn(II) tags for DEER distance measurements in proteins via C-S attachment

Received 00th January 20xx,
Accepted 00th January 20xx

DOI: 10.1039/x0xx00000x
www.rsc.org/

Andrea Martorana[a,&], Yin Yang[b,&], Yu Zhao[b], Qing-Feng Li[b], Xun-Cheng Su[b]* and Daniella Goldfarb[a]*

Mn^{2+} chelating tags for Mn^{2+}-Mn^{2+} distance measurements by pulse EPR spectroscopy were developed. They feature a stable C-S conjugation to the protein, high reactivity towards cysteine thiols and short and rigid linkers that can be used in distance measurement with high resolution under reductive conditions. Double electron-electron resonance measurements at 95 GHz on ubiquitin labeled with these tags showed the expected narrow distance distribution.

Pulse dipolar EPR spectroscopy, in particular, the double electron-electron resonance (DEER) experiment[1, 2], has emerged in the last decade as a powerful method in structural biology because it provides distance distributions between well-defined sites within bio-macromolecules. It is based on measuring the dipolar interactions between two paramagnetic centers, and it can access distances in the range of 1.5-8 nm in frozen solutions.[3, 4] Because most proteins do not contain paramagnetic centers, this methodology relies on introducing spin labels through techniques of site-directed spin labeling (SDSL).[5] The most widely used method is the attachment of a pair of derivatives of nitroxide stable radicals to native or genetically engineered cysteine residues through the formation of disulfide (S-S) bonds. Metal ions can also be used as spin labels, such as Cu(II) at X-band frequencies[6]. Gd^{3+} (S=7/2) spin labels have been recently introduced for DEER measurement at frequencies higher than the standard X-band (~9.5 GHz), namely, Q- and W-band (~32 and ~95 GHz) frequencies, featuring advantages in terms of sensitivity, lack of orientation selection and chemical stability.[7, 8] Such measurements were reported for model compounds[9-11], proteins[12-14], peptides in solutions[15] and membranes[16, 17], DNA[18] and nanoparticles.[19] Recently, a set of Gd^{3+} ruler molecules, with Gd^{3+}-Gd^{3+} distances in the range of 2.1-8.5 nm, have been used to substantiate the validity of data analysis for this family of high-spin labels.[11]

The Mn^{2+} ion is a half integer high-spin ion that is characterised by high EPR sensitivity at high fields, similar to Gd^{3+}, and it can potentially become a useful spin label for distance measurements as well. To date, there has been only one report of Mn^{2+}-Mn^{2+} distance measurement in a protein[20] using an EDTA-Mn^{2+} spin label, and recently such distance measurements were demonstrated on a model peptide in solution using a maleimide-DO3A Mn^{2+} label.[21] Both measurements were carried out at W-band. Mn^{2+}-nitroxide distance measurements were reported as well.[22, 23]

One of the motivations for developing the approach of Gd^{3+} spin labeling for distance measurements is its suitability for *in-cell* DEER applications, which holds considerable promise because it will allow proteins to be probed in their native environment.[24, 25] The ideal spin label for distance measurements in proteins should have the following characteristics: (i) efficient conjugation to the protein without disturbing the protein's structure; (ii) low flexibility of the attached spin label, which yields a narrow distance distribution, thus providing accurate distances and high sensitivity to small conformational variations in the protein; and (iii) high EPR sensitivity. In the case of metal ion-based spin labels, a high affinity of the chelating moiety to the metal ions is essential. When *in-cell* measurements are involved, the chemical stability of the paramagnetic entity and the linker to the protein become crucial factors.

Unfortunately, the standard nitroxide spin labels are reduced in the cell,[26, 27] and similarly, the common conjugation via the formation of S-S bonds with a cysteine residue is not appropriate because of their reduction in the cell.[26] The low stability of the paramagnetic entity can be overcome by the use of Gd^{3+},[24, 25] and probably also Mn^{2+}, although Mn^{2+}-Mn^{2+} in cell distance measurements have not yet been demonstrated. The conjugation stability can be addressed by replacing the S-S bond with a more chemically stable C-S bond. Popular reagents use maleimides[24, 26], where the thiolether tether of the C-S bond bridging the protein and spin label is stable under reductive conditions, and it is not hydrolyzed or reduced in cytoplasmic compartments. The downsides of maleimide derivatives tags are as follows: (i) they can also react with side chain amino groups of lysine; (ii) maleimide derivative tags are not stable at lower pHs due to hydrolysis; (iii) when a maleimide derivative tag reacts with a cysteine a new chiral center is generated, which leads to diastereomeric protein–tag conjugates[28]. Finally (iv), their tether is relatively long and flexible and this leads to a broad distance distribution. Vinyl groups attached to pyridine rings also work and they provide a shorter linker.[25, 28, 29]

[a] Department of Chemical Physics, Weizmann Institute of Science, Rehovot 76100 (Israel). Email: daniella.goldfarb@weizmann.ac.il
[b] State Key Laboratory of Elemento-organic Chemistry, Collaborative Innovation Center of Chemical Science and Engineering (Tianjin), Nankai University, Tianjin 300071, China. Email: xunchengsu@nankai.edu.cn
[c] -[&] equal contribution.

† Footnotes relating to the title and/or authors should appear here.
Electronic Supplementary Information (ESI) available: [details of any supplementary information available should be included here]. See DOI: 10.1039/x0xx00000x

In this work we introduce three new tags, namely, L1, L2, and L3 (see Fig. 1) for Mn^{2+}-Mn^{2+} distance measurements that form a C-S conjugation with cysteine residues in the protein and short linkers.

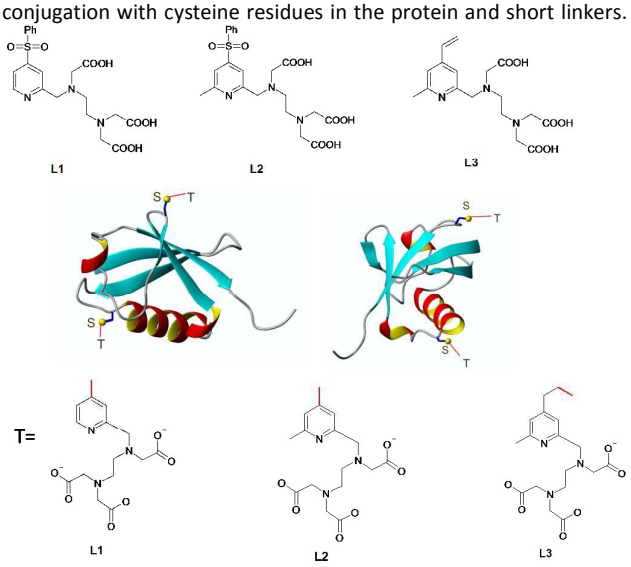

Figure 1. The structure of the tags used for protein labeling (top); the ribbon structure of the two human ubiquitin mutants, T22C/G47C (left) and G35C/E64C (right) (PDB code 1UBQ) (middle). Chelate structures showing the new bond (in red) that was created after conjugation (bottom).

We demonstrate their performance on two ubiquitin mutants (see Fig.1). Ubiquitin was chosen because it is an extensively used model with a known structure and labelling at T22,G47 G35 and E64 are known not to disturb the structure[28, 30] The new tags consist of a potentially high binding-affinity metal chelator, N-(pyrid-2-yl-methyl)ethylenediamine-N,N',N'-triacetic acid (PEDTA),[31] and a thiol specific reactive group. The crystal structures of PEDTA with Fe^{3+} and Cu^{2+} show coordination to two amino-nitrogen atoms, the pyridine nitrogen atom, and two carboxylic groups.[32] Therefore, we expect a similar binding coordination for Mn^{2+} to PEDTA and a high affinity. Of a particular interest are L1 and L2 because of their higher reactivity towards protein thiols as compared with previously reported vinyl groups used in 4VPyMTA[30] and 4PS_PyMTA[33] tags (like L3). The stable C-S linker is stable in reductive conditions and thus can be applied in distance measurement by EPR in the presence of reducing reagents. In addition, they produce a shorter and more rigid linker between the protein backbone and the Mn^{2+} ion, which restricts the flexibility of the spin labels and reduces the spin label-dependent contribution to the distance distributions derived from DEER measurements.

The synthesis of the tags and the procedure for protein conjugation are described in detail in the ESI. NMR spectra of the two mutants with the ligated tags (without Mn^{2+}) showed that the labeling does not alter the protein's structure significantly because the chemical shift perturbations are in a narrow range centered in those residues close to the ligation sites (see ESI Figs. S2-S3). The ligation yield of the doubly-labeled protein was about 70% after protein purification by an ion exchange column. High ligation yields are important for DEER experiments because poor yields enhance the background decay owing to non-specific intermolecular interactions and reduce the DEER effects due to intramolecular interactions.

The protein samples were first prepared by titration of 0.1 mM protein-tag with 1.8 equivalents of $MnSO_4$ in 20 mM MES buffer at pH 6.4 and then were lyophilized. The protein powder was redissolved in D_2O/glycerol-d_8 (7:3, volume/volume) at about 0.1 mM, and the protein solution (about 3 μL) was loaded into quartz capillaries (0.84 mm outer diameter, 0.60 mm inner diameter) for DEER measurements.

The W-band echo detected (ED) the EPR spectra of T22C/G47C-L1-Mn^{2+}, L2-Mn^{2+} and L3-Mn^{2+}, in the region of the central transition, are depicted in Figure 2a. The spectra reveal the characteristic six peaks for Mn^{2+} owing to the hyperfine coupling with the ^{55}Mn nucleus (I=5/2)The spectra of the G35C/E64C L1-Mn^{2+} and L2-Mn^{2+} samples are similar to those of the corresponding T22C/G47C samples (see Fig. 2b). These spectra, although narrower than those with the EDTA tag,[20] are still broader than those of maleimide-DO3A-Mn^{2+},[21] thus compromising sensitivity. Typical echo decay curves are presented in Fig. S4, showing that echoes can be detected up to 15 μs at 10K.

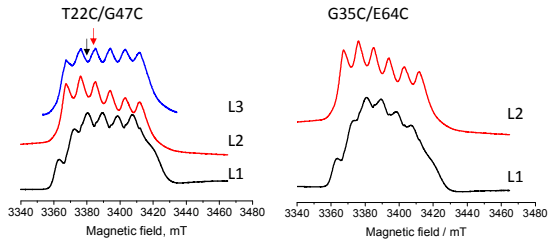

Figure 2. W-band ED-EPR spectra (10K) of the doubly Mn^{2+}-labeled ubiquitin mutants. The positions of the pump (ν_2, red) and the observed pulses (ν_1, black) in the DEER measurements are specified as arrows in the left panel. The spectra were recorded with π/2 and π pulses of 30 and 60 ns, respectively, and a τ value of 750 ns.

DEER data were recorded at 10 K using a W-band home-built spectrometer[34] with the four-pulse sequence: π/2 - τ - π -τ-τ_1- π - τ_1- echo, at frequency ν_1, and a π pulse at frequency ν_2 positioned at a variable time *t* after the first of the two π pulses at ν_1.[2] t=0 correspond to a time τ after the first π pulse and it was varied from t=-200 ns to τ_1-500 ns. The frequency set-up of the pump pulse (ν_2) and the observed pulses (ν_1) within the spectrum, separated by 90 MHz, is shown in Fig. 2. The length of the pump pulse, t_{pump}, was 15 ns, the length of the π/2 observer pulse, $t_{observer, \pi/2}$, was 15 ns, and the length of the π observer pulse, $t_{observer, \pi}$, was 30 ns. The delay time, τ, was 400 ns, the step of *t* was 15 ns, and the repetition time was 700 μs. The accumulation time ranged from 2 to 6 h. Full transient echo traces were collected for each *t* value in the DEER sequence and the echo integration was carried out after data collection. The integration gate was chosen to obtain the best signal-to-noise ratio and usually was found to be equal to the echo's full width at half height. Data analysis was carried out with DeerAnalysis[35] and Tikhonov regularization.

Figure 3a shows the DEER traces after background removal for T22C/G47C with L1-Mn^{2+}, L2-Mn^{2+} and L3-Mn^{2+} (the primary DEER data are given in Fig. S5. All three tags exhibit a modulation depth (λ ~ 0.7-1%), which is lower than what is usually observed for Gd^{3+} under these experimental conditions. This is expected considering the EPR spectral width of Mn^{2+} and the splitting into 6 hyperfine components. The λ value is twice as high as compared with the EDTA tags[20], and about twice lower than DOTA-derived tags[21], all of which is in agreement with the EPR spectral width. The distance distributions are shown in Fig. 3b. The trend observed for the maxima of the distance distribution (3.1-3.2 nm) is L1~ L2< L3 and L2≤L1<L3 for the distance distribution width at half height. Because of the broad EPR lines, significant contributions to the distance

distributions arising from ignoring the pseudosecular terms of the dipolar interaction in the analysis are not expected.[11, 21] The results for the G35C/E64C mutant with L1 and L2 are shown in Fig. 3cd. The Mn^{2+}-Mn^{2+} distances for L1 and L2 are similar, 3 nm, with L2 exhibiting a significantly narrower distance distribution. The modulation depth was around 0.6-0.8 %. All these characteristics are summarized in Table 1.

Both T22C/G47C-L2-Mn^{2+} and T22C/G47C-L1-Mn^{2+} exhibit a narrower distance distribution than do the G35C/E64C corresponding samples. This is in excellent agreement with the flexibility of the residue, which is modified by the spin label. Residue E64 resides in a flexible loop, whereas residues T22, G35 and G47 are located close to the rigid secondary structural segment. This shows that the rigidity of the tags allows one to derive information on the protein not only from the distance but also from the width of the distance information.

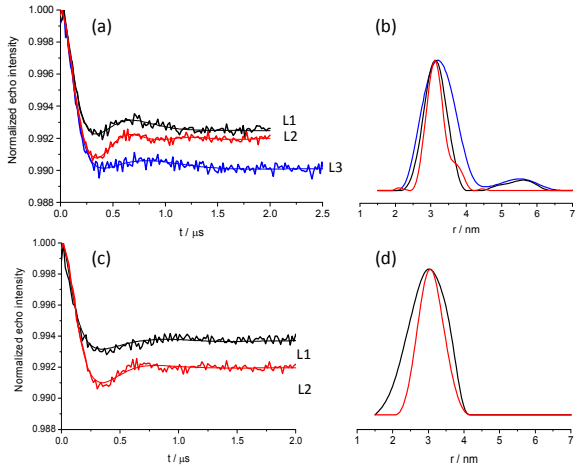

Figure 3. (a) Background corrected W-band DEER traces for T22C/G47C with L1-Mn^{2+} (black), L2- Mn^{2+} (red) and L3- Mn^{2+} (blue) along with the fit obtained with the distance distribution shown in (b). (c) and (d) the same as (a) and (b) for G35C/E64C with L1-Mn^{2+} (black), L2- Mn^{2+} (red).

The coordination sphere of Mn^{2+} is expected to be the same for L2 and L3; they differ only in the length of the conjugating tether to the protein, with L3 having a tether longer by two CH_2 groups. This should result in higher flexibility and possibly also in a somewhat longer distance, as was indeed observed for T22C/G47C. Actually, it is rather remarkable that such subtleties were resolved in the DEER measurements. These results are consistent with an earlier analysis by paramagnetic NMR spectroscopy which showed that the paramagnetic tensor determined for the lanthanide complex of ubiquitin G47C-4PSPyMTA[33], an analogue of L1 and L2, is six times larger than that of ubiquitin G47C-4VPyMTA[30], an analogue of L3. The shorter and more rigid the linker between the protein and the spin label is, the larger are the paramagnetic effects on proteins. This suggests that the distance distribution width derived from the DEER experiment shares similar concepts with paramagnetic NMR spectroscopy, where the flexibility of the tag itself and the ligation site (the protein) contribute to the paramagnetic effects on proteins. Therefore, site-specific paramagnetic tagging proteins for paramagnetic NMR spectroscopy provide an efficient way of predicting narrow distance distributions by DEER measurements.

The L1 and L2 tags have the same ligation tether and indeed they exhibit the same distance in terms of the maximum distance distribution. However, unexpectedly, they do differ in the width of the distance distribution for both mutants, with L2 exhibiting a narrower distribution. Although the difference for T22C/G47C is small and can be considered within the error limit, it is significant for G35C/E64C. The only difference between the two tags is the methyl group in the *meta* position in the pyridine group in L2. In general, L2 exhibited a higher reactivity towards the protein thiol than did L1 with both ubiquitin mutants. The methyl group can also lead to small differences in the Mn^{2+} coordination environment, which is supported by the different ED-EPR spectra of T22C/G147C-L1-Mn^{2+} and T22C/G147C-L2-Mn^{2+}. The EPR spectrum of Mn^{2+} is determined by the ^{55}Mn isotropic hyperfine interaction and the zero field splitting (ZFS) parameters D and E. These parameters are sensitive to the local symmetry around the Mn^{2+} ion, with D being sensitive to axial distortions and E to rhombic distortions. Simulations (see ESI and Fig. S6 for details) of the T22C/G47C-L1-Mn^{2+} spectrum (using Easyspin[36]), limited to the central transition region, yielded a satisfactory fit with D and E values of 3060 MHz and 459 MHz, respectively. In contrast, simulations of the analogous L2 spectrum did not result in a very good fit. The width and positions of the hyperfine component could be reproduced with D and E values of 1920 and 576 MHz, respectively, but not their relative intensities. This suggests that more than one Mn^{2+} species contribute to the L2 spectra.. To substantiate these findings, full range ED-EPR spectra of Mn^{2+} bound to the tag alone, with L1 and L2 in excess (1:1.66), were measured and simulations confirmed that the D value for L1 is indeed larger than for L2 (see Fig. S6 and Table S1), indicating that the Mn^{2+} in the L1 complex experiences a higher axial distortion. The relative intensity of the sextet components of the central transition of L1-Mn^{2+} did agree with the simulations, consistent with the suggestion that free Mn^{2+} or other species, may contribute to the spectra of T22C/G47C-L2-Mn^{2+} and G35C/E64C- L2-Mn^{2+} . The D value of L1-Mn^{2+} is relatively high compared to that of other Mn $^{2+}$ complexes of biological relevance and is comparable to that of Mn^{2+}-EDTA.[37]

To further rationalize the structural differences in the coordination sphere of Mn^{2+} with L1 and L2 and to verify whether the methyl group can affect the coordination of pyridine nitrogen to Mn^{2+}, we carried out ELDOR (electron-electron double resonance) detected NMR[38] measurements on Mn^{2+}-L1 and Mn^{2+}-L2. It is the coordination of Mn^{2+} to pyridine that lends significant rigidity to the tag, manifested by a narrow distance distribution and shorter distances, as compared with non-coordinated pyridine nitrogen. The spectra of these two complexes, shown in Fig. S7, are very similar, both in terms of frequencies and intensities,[39] thus indicating that they are bound to the same number and types of ^{14}N nuclei with a hyperfine coupling of 1.9 MHz. Therefore, we can conclude that pyridine ^{14}N is coordinated, consistent with the narrow distance distribution for L2 and L1 for T22C/G47C and with the crystal structures of PEDTA with Cu^{2+} and Fe^{3+} .[32] It is therefore likely that the narrower distance distribution of L2 arises from some steric hindrance induced by the methyl group, which limits the mobility of the tag when it is attached to G35C/E64C.

We also explored the affinity of Mn^{2+} to L1 and L2 by NMR and EPR measurements, which are summarized in the ESI (Figs. S8-S12). These measurements show that the binding affinity to L1 is larger than L2, namely, that the methyl group does affect the binding affinity; it lowers it. Moreover, the binding affinity is pH dependent, as expected, and it is higher at high pH values, like for EDTA, but it was found to be lower than that of EDTA. We expect the binding constant of Mn^{2+} to the tags attached to the protein to be higher than for the tag alone because of the electron withdrawing

characteristics of the phenylsulfone group, which should decrease the binding strength of the pyridine to the metal ion. Nonetheless, the binding constant of Mn^{2+} to T22C/G47C-L1 was found to be insufficient for *in cell* DEER measurements. Such measurements carried out under the same conditions as reported earlier,[24] showed that the *in cell* ED-EPR spectrum changed to a sextet with sharp lines, a sign that the majority of the Mn^{2+} is no longer coordinated to L1. This indicates that the binding affinity is not sufficiently high to compete with the many endogenous binding sites of various cell components. This calls for further development of high-affinity Mn^{2+} tags for *in cell* Mn^{2+} DEER measurements.

To summarize, we presented three new tags for Mn^{2+} -Mn^{2+} distance measurements, featuring a small size and stable C-S protein conjugation. Two of them, L1 and L2, also have a short and rigid tether and high reactivity towards thiol groups of cysteine residue, which make them highly attractive for *in-vitro* DEER studies. Although their EPR spectra are broader than that of the maleimide-DOTA tag[21], which yields broad distance distributions, yielding lower modulation depths, their DEER traces could be collected within several hours and they provided a narrow distance distribution.

Acknowledgments

This work was supported by the Israel Science Foundation, F.I.R.S.T program, MOST (2013CB910200) and NSFC (21473095 and 21273121). We thank Dr. Alexej Litvinov for his help with the ELDOR-detected NMR spectra. D. G. holds the Erich Klieger Professorial Chair in Physical Chemistry.

Table 1. Parameters of ubiquitin mutant-tag (L1, L2 or L3) conjugates complexed with Mn^{2+}, determined by DEER experiment

Sample	λ%	Distance[a] (nm)	Width[b] (nm)
T22C/G47C			
L1-Mn	0.75	3.1	0.8[c]
L2-Mn	0.8	3.1	0.6
L3-Mn	1.0	3.2	1.2
G35C/E64C			
L1-Mn	0.6	3.0	1.3
L2-Mn	0.8	3.0	0.8

[a] Maximum of distance distribution. [b] Full-width half-height. [c] For comparison, the width of a model α-helix peptide with a maleimide-DO3A tag was 1.3 nm [21] and an EDTA tag with a protein had a width of ~1.5 nm.[20]

1. A. D. Milov, A. B. Ponomarev and Y. D. Tsvetkov, *Chem. Phys. Lett.*, 1984, **110**, 67-72.
2. M. Pannier, S. Veit, A. Godt, G. Jeschke and H. W. Spiess, *J. Magn. Reson.*, 2000, **142**, 331-340.
3. P. P. Borbat and J. H. Freed in *Struct. Bond.*, eds. C. Timmel and J. Harmer, Springer Berlin Heidelberg, 2013, vol. 152, pp. 1-82.
4. G. Jeschke and Y. Polyhach, *Phys. Chem. Chem. Phys.*, 2007, **9**, 1895-1910.
5. W. L. Hubbell, A. Gross, R. Langen and M. A. Lietzow, *Curr. Opin. Struct. Biol.*, 1998, **8**, 649-656.
6. T. F. Cunningham, M. R. Putterman, A. Desai, W. S. Horne and S. Saxena, *Angew. Chem.-Intl Ed.*, 2015, **54**, 6330-6334.
7. D. Goldfarb, *Phys. Chem. Chem. Phys.*, 2014, **16**, 9685-9699.
8. A. Feintuch, G. Otting and D. Goldfarb, in *Methods Enzymol.*, Academic Press, 2015, DOI: http://dx.doi.org/10.1016/bs.mie.2015.07.006.
9. A. M. Raitsimring, C. Gunanathan, A. Potapov, I. Efremenko, J. M. L. Martin, D. Milstein and D. Goldfarb, *J. Am. Chem. Soc.*, 2007, **129**, 14138-14140.
10. A. Potapov, Y. Song, T. J. Meade, D. Goldfarb, A. V. Astashkin and A. Raitsimring, *J. Magn. Reson.*, 2010, **205**, 38-49.
11. A. Dalaloyan, M. Qi, R. Ruthstein, S. Vega, A. Godt, A. Feintuch and D. Goldfarb, *Phys. Chem. Chem. Phys.*, 2015.
12. A. Potapov, H. Yagi, T. Huber, S. Jergic, N. E. Dixon, G. Otting and D. Goldfarb, *J. Am. Chem. Soc.*, 2010, **132**, 9040-9048.
13. H. Yagi, D. Banerjee, B. Graham, T. Huber, D. Goldfarb and O. Gottfried, *J. Am. Chem. Soc.*, 2011, **133**, 10418-10421
14. D. T. Edwards, T. Huber, S. Hussain, K. M. Stone, M. Kinnebrew, I. Kaminker, E. Matalon, M. S. Sherwin, D. Goldfarb and S. Han, *Structure*, 2014, **22**, 1677-1686.
15. M. Gordon – Grossman, I. Kaminker, Y. Gofman, Y. Shai and D. Goldfarb, *Phys. Chem. Chem. Phys.*, 2011, **13**, 10771-10780.
16. E. Matalon, T. Huber, G. Hagelueken, B. Graham, A. Feintuch, V. Frydman, G. Otting and D. Goldfarb, *Angew. Chem. Int. Ed.*, 2013, **52,** 11831-11834.
17. N. Manukovsky, V. Frydman and D. Goldfarb, *J. Phys. Chem. B.*, 2015, **119,**13732-3741.
18. Y. Song, T. J. Meade, A. V. Astashkin, E. L. Klein, J. H. Enemark and A. Raitsimring, *J. Magn. Reson.*, 2011, **210** 59-68
19. M. Yulikov, P. Lueders, M. F. Warsi, V. Chechik and G. Jeschke, *Phys. Chem. Chem. Phys.*, 2012, **14**, 10732-10746.
20. D. Banerjee, H. Yagi, T. Huber, G. Otting and D. Goldfarb, *J. Phys. Chem. Lett.*, 2012, **3**, 157-160.
21. H. Y. Vincent Ching, P. Demay-Drouhard, H. C. Bertrand, C. Policar, L. C. Tabares and S. Un, *Phys. Chem. Chem. Phys.*, 2015, DOI: 10.1039/C5CP03487F.
22. D. Akhmetzyanov, J. Plackmeyer, B. Endeward, V. Denysenkov and T. F. Prisner, *Physical chemistry chemical physics : PCCP*, 2015, **17**, 6760-6766.
23. I. Kaminker, M. Bye, N. Mendelman, K. Gislason, S. T. Sigurdsson and D. Goldfarb, *Phys. Chem. Chem. Phys.*, 2015, **17**, 15098-15102.
24. A. Martorana, G. Bellapadrona, A. Feintuch, E. Di Gregorio, S. Aime and D. Goldfarb, *J. Am. Chem. Soc.* , 2014, **136** 13458-13465
25. M. Qi, A. Gross, G. Jeschke, A. Godt and M. Drescher, *J. Am. Chem. Soc.*, 2014, **136**, 15366-15378.
26. R. Igarashi, T. Sakai, H. Hara, T. Tenno, T. Tanaka, H. Tochio and M. Shirakawa, *J. Am. Chem. Soc.*, 2010, **132**, 8228-+.
27. I. Krstic, R. Haensel, O. Romainczyk, J. W. Engels, V. Doetsch and T. F. Prisner, *Angew. Chem. Intl. Ed.*, 2011, **50**, 5070-5074.
28. Li Q.-F., Yang Y., Maleckis A., G. Otting and X.-C. Su, *Chem. Commun.*, 2012, **48**, 2704-2706.

29. F. H. Ma, J. L. Chen, Q. F. Li, H. H. Zuo, F. Huang and X. C. Su, *Chem. Asian. J.*, 2014, **9**, 1808-1816.
30. Y. Yang, Q. F. Li, C. Cao, F. Huang and X. C. Su, *Chem. Eur. J*, 2013, **19**, 1097-1103.
31. R. Ruloff, L. Beyer, F. Dietze, K. Arnold, W. Gründer and M. Wagner, *Z. Anorg. Allg. Chem*, 1995, **621**, 807-811.
32. R. Richter, C. Kuntert, R. Ruloff and L. Beyer, *Z. Anorg. Allg. Chem*, 1996, **622**, 707-712.
33. Y. Yang, J. T. Wang, Y. Y. Pei and X. C. Su, *Chem. Commun.*, 2015, **51**, 2824-2827.
34. D. Goldfarb, Y. Lipkin, A. Potapov, Y. Gorodetsky, B. Epel, A. M. Raitsimring, M. Radoul and I. Kaminker, *J. Magn. Reson.*, 2008, **194**, 8-15.
35. G. Jeschke, V. Chechik, P. Ionita, A. Godt, H. Zimmermann, J. Banham, C. R. Timmel, D. Hilger and H. Jung, *Appl. Magn. Reson.*, 2006, **30**, 473-498.
36. S. Stoll and A. Schweiger, *J. Magn. Reson.*, 2006, **178**, 42-55.
37. T. A. Stich, S. Lahiri, G. Yeagle, M. Dicus, M. Brynda, A. Gunn, C. Aznar, V. J. DeRose and R. D. Britt, *Appl. Magn. Reson.*, 2007, **31**, 321-341.
38. P. Schosseler, T. Wacker and A. Schweiger, *Chem. Phys. Lett.*, 1994, **224**, 319-324.
39. E. M. Bruch, M. T. Warner, S. Thomine, L. C. Tabares and S. Un, *J. Phys. Chem. B*, 2015, DOI: 10.1021/acs.jpcb.5b01624.

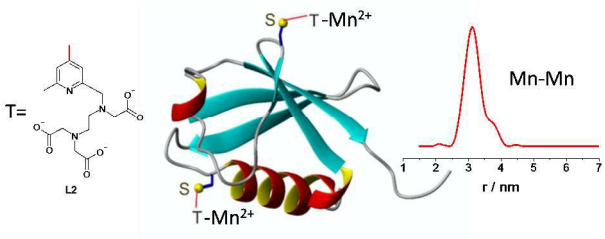

Tags for Mn^{2+} -Mn^{2+} distance measurements in proteins with a short linker that generate narrow distance distributions were developed